LIMNOLOGY
and
OCEANOGRAPHY: METHODS

ASLO

Limnol. Oceanogr.: Methods 15, 2017, 38–53

doi: 10.1002/lom3.10140

A novel membrane inlet-infrared gas analysis (MI-IRGA) system for monitoring of seawater carbonate system

Emma F. Camp,[1,2] Laing F. Dong,[1] David J. Suggett,[1,2] David J. Smith,[1] Tobias G. Boatman,[1] Joseph R. Crosswell,[2] Christian Evenhuis,[2] Steven Scorfield,[1] Amit Walinjkar,[3] John Woods,[3] Tracy Lawson[1]*

[1]School of Biological Sciences, University of Essex, Wivenhoe Park, Colchester, Essex, UK
[2]Climate Change Cluster (C3), University of Technology Sydney, Broadway, New South Wales, Australia
[3]School of Computing and Engineering, University of Essex, Wivenhoe Park, Colchester, Essex, UK

Abstract

Increased atmospheric CO_2 concentrations are driving changes in ocean chemistry at unprecedented rates resulting in ocean acidification, which is predicted to impact the functioning of marine biota, in particular of marine calcifiers. However, the precise understanding of such impacts relies on an analytical system that determines the mechanisms and impact of elevated pCO_2 on the physiology of organisms at scales from species to entire communities. Recent work has highlighted the need within experiments to control all aspects of the carbonate system to resolve the role of different inorganic carbon species on the physiological responses observed across taxa in real-time. Presently however, there are limited options available for continuous quantification of physiological responses, coupled with real-time calculation of the seawater carbonate chemistry system within microcosm environments. Here, we describe and characterise the performance of a novel pCO_2 membrane equilibrium system (the Membrane Inlet Infra-Red Gas Analyser, MI-IRGA) integrated with a continuous pH and oxygen monitoring platform. The system can detect changes in the seawater carbonate chemistry and determine organism physiological responses, while providing the user with real-time control over the microcosm system. We evaluate the systems control, response time and associated error, and demonstrate the flexibility of the system to operate under field conditions and within a laboratory. We use the system to measure physiological parameters (photosynthesis and respiration) for the corals *Pocillipora damicornis* and *Porites cylindrica*; in doing so we present a novel dataset examining the interactive role of temperature, light and pCO_2 on the physiology of *P. cylindrica*.

Atmospheric carbon dioxide (CO_2) concentrations are continuing to rise at an unprecedented rate, lowering global surface seawater pH, which is commonly referred to as ocean acidification (Khatiwala et al. 2013). Studying the impacts of ocean acidification on marine organisms has become a major global research focus. Collectively, research to-date provides compelling evidence that by the end of the century ocean acidification will impact marine communities and entire ecosystem structures, largely through a loss of productivity, growth, and/or fecundity of many key species (Fabry et al. 2008; Kroeker et al. 2010, 2013; Riebesell and Gattuso 2015).

Three main approaches have been adopted to study the impacts of ocean acidification: (1) examining *in situ* natural pH gradients, (2) *in situ* field mesocosm studies, and (3) conducting controlled laboratory experiments. Intensive research examining present day natural pH/pCO_2 (partial pressure of CO_2) gradients have been particularly important in gaining insight into ecosystem level responses under future acidification conditions. However, the need to specifically examine the interactions of both local (e.g., light and nutrient availability) and global (e.g., warming) environmental variables predicted to change alongside pH, has led to an increased need to improve experimental control, so that globally relevant biogeochemical and ecological responses can be more accurately studied. The need for controlled experiments has been a primary driver for technological innovation to not only measure pCO_2, but also manipulate and control pCO_2 within experimental treatments.

*Correspondence: tlawson@essex.ac.uk

C.E.F and D.L.F are joint lead authors.

Additional Supporting Information may be found in the online version of this article.

Microcosms are a favored experimental approach to examine the response of single species, as well as different species assemblages to ocean acidification, in both open and closed systems (Stewart et al. 2013). Microcosms have been used to study a range of individual taxa (e.g., corals Dove et al. 2013; Suggett et al. 2013), sea anemones (Suggett et al. 2012), microalgae (Sciandra et al. 2003; Leonardos and Geider 2005), seagrass and macroalgae (Koch et al. 2013), over varying timeframes (days: Comeau et al. 2014, or months: Collins and Bell 2004; Anthony et al. 2008). Whole communities have also been investigated, both *in situ* (Campbell and Fourqurean 2011; Gattuso et al. 2014) and within open (Moya et al. 2008) and closed (Anthony et al. 2008) laboratory systems, with recent advances superimposing treatment conditions onto natural diel cycles (Dove et al. 2013; Jokiel et al. 2014; Camp et al. 2016a). Conditions have been manipulated to recreate conditions predicted under future climate change using a variety of approaches, which primarily include: acid/base manipulation (e.g., Richier et al. 2014; Camp et al. 2016a), the use of premixed commercial gases (e.g., Talmage and Gobler 2009; Yamamoto et al. 2012), or a mix of pure CO_2 with ambient air to achieve a desired pCO_2 level (e.g., Byrne et al. 2010; Fangue et al. 2010). Evaluation of these various methods have found negligible differences (Gattuso and Lavigne 2009). Fundamentally however, all of these microcosm experiments desire to accurately measure, control and/or manipulate the seawater carbonate system.

A number of experimental systems have already been developed to provide the capacity to control both the carbonate chemistry and other bio-physiochemical variables of microcosm environments (Leonardos and Geider 2005; Gattuso et al. 2014). For example, Coelho et al. (2013) describe an experimental life support system that allows multiple stressors to be tested alongside the carbonate chemistry, which is controlled by CO_2 bubbling and a pH probe and controller. The system however does not allow user control based on real-time estimates of unmeasured carbonate parameters. Another system, the Multiple Stressor Experimental Aquarium at Scripps (MSEAS; Bockmon et al. 2013) assumes alkalinity to remain constant, despite the fact that alkalinity varies across marine systems. The dissolved inorganic carbon (DIC) is controlled by mole fraction CO_2 gas additions and using the same principle, the concentration of oxygen ($[O_2]$) is simultaneously controlled, with temperature controlled using a water bath. The system uses a membrane contactor, which requires filtering and pumping of water and thus is unlikely to be suitable for naturally-turbid waters or phytoplankton studies. Presently, no "one-size fits all" control system exists for microcosm experiments.

Here, we described a new variant of a microcosm system developed to monitor organism responses to changes in pCO_2, temperature and light. In contrast to previous designs, the system allows real-time calculation of the full carbonate chemistry system, from direct measurements of pH, temperature, salinity, and pCO_2, using a novel membrane inlet gas exchange apparatus connected to an infra-red gas analyser (the Membrane Inlet-Infra Red Gas Analyser, MI-IRGA). Direct $[O_2]$ measurements also allow physiological responses to be simultaneously quantified and the system can be configured to control O_2 levels by a solenoid feedback system. Real-time data acquisition provides the user with the capacity to manipulate the microcosm environment. User-defined conditions provide precise control over pCO_2 and allow instantaneous calculation of the carbonate chemistry system using the custom-designed computer software (CCS). The system can be allowed to drift in response to metabolic activity or, experimental conditions can be kept constant by compensating for the biologically mediated response, thus making experimentation much more comparable to real world conditions.

Materials and procedures

Microcosm design

The microcosm was based on a modified pH-stat system developed previously to grow calcifying phytoplankton at high biomass, but under tightly controlled pH scenarios (*see* Leonardos 2008; Brading et al. 2011). The microcosm (Fig. 1) comprised of a water-jacketed vessel (1 L capacity) sealed with a Teflon lid, with ports for probe and sampling access (Supporting Information Fig. 1). For sessile organisms such as corals, seawater was supplied to the microcosm via a continuous flow system, using a peristaltic pump with a flow rate of 4 L min^{-1}, from the aquarium tanks in the Coral Reef Research Unit at the University of Essex (*see* Suggett et al. 2013). However, supply to the microcosms was switched off for metabolic incubations to form a closed-system.

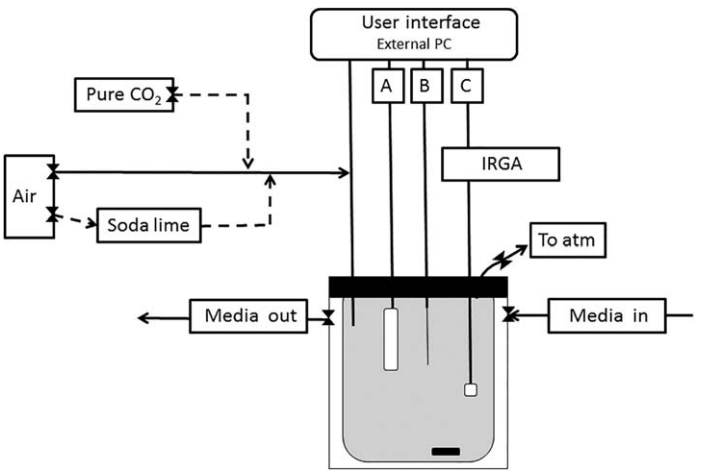

Fig. 1. Schematic diagram of the MI-IRGA system. The microcosm is comprised of a water-jacketed reactor vessel containing a stir bar. A series of probes are inserted into the microcosm. A pH probe (**A**) is used for measurement of total pH (pH_T), and an optical measurement is used to quantify O_2 (**B**). The CO_2 exchange system enables continuous monitoring of pCO_2 via an IRGA and customised pCO_2 probe (**C**); pCO_2 can be controlled to a desired level in a feedback system, which switches values between CO_2 free (stripped with soda lime) or CO_2 enriched air (from a pure CO_2 cylinder) as indicated by the dashed lines in the schematic. The microcosm can operate in an open or closed configuration.

A sensor array was used to measure microcosm conditions. An optical O_2 sensor (Optode system, Ocean optics Ltd) measured [O_2] with an accuracy and precision of 0.05 μmol L^{-1}. Temperature was measured using a NeoFox TB probe with an accuracy and precision of 0.01°C. Conductivity was measured using a Dura probe (Ross Ultra; Fisher Scientific, UK) and converted to salinity within the in-house computer software (CCS) system using the equations in UNESCO (1983). pH was measured using a glass Triode Combination Electrode (Ross Ultra; Fisher Scientific, UK) calibrated with TRIS buffers (7.5–9.0, made following Carbon Dioxide Information Analysis Centre (CDIAC) protocols) to measure pH in total scale (pH_T) (Dickson et al. 2007). Based on manufacturer-reported specifications the pH system was accurate to $\pm$ 0.01 pH units, with a drift of $<$ 0.002 pH d^{-1}. A custom designed gas exchanger unit attached to an infra-red gas analyser (LI-820 CO_2 Gas analyser; LI-COR, UK) continuously measured the mole fraction of CO_2 (xCO_2) in recirculated carrier gas. The IRGA xCO_2 measurement had an accuracy of $\pm$ 0.5% in dry air, $\pm$ 1.5% in humidified air and drift of $<$ 1 ppm d^{-1} when configured for a measurement range of 0–1000 ppm, as used in this study. Discrete water samples were collected from the microcosm, from which total alkalinity (A_T) was determined by an open-cell potentiometric titration using a Titrino titrator (model 848; Metrohm, UK). 0.1 N standardised Hydrochloric acid was used and A_T was measured with an accuracy and precision of ca. $\leq$ 2 μmol kg^{-1}, as verified with certified reference materials distributed by A. Dickson (Scripps Institute of Oceanography). Microcosms were maintained in a water bath to control temperature using NeoHeaters (IPX8; Aquael, Poland), however the pH-stat system has been previously used in a climate controlled room (*see* Brading et al. 2011). Lighting for the system was supplied externally 24 volt cool white LEDS (Daylights, Farnell, UK).

Membrane gas exchanger unit

The membrane inlet was comprised of a Teflon housing for a silicon membrane exchanger unit configured in a "spaghetti" set-up (Fig. 2) of 0.3 mm bore, 80 mm long, gas/CO_2 permeable platinum cured silicone tubes (Cole-Palmer Instrument Company, UK). All tubes were attached to both ends (hollow disks machined from Teflon) of the housing via 0.5 mm diameter syringe needles. The hollow disk at one end collected all of the air from the tubes to the IRGA, while the remaining end connected to a disk that returned gas from the IRGA. An O-ring gasket was used to provide a water impermeable seal. Gas streams from the tubes converge at a central air space before leaving the probe through an outlet tube. Air was used as the carrier gas and continuously recirculated in a closed loop between the IRGA and probe, at a flow rate of approximately 0.3 L min^{-1} (Fig. 2). In order to convert xCO_2 data to pCO_2, it was assumed that the carrier gas was humidified and at an ambient atmospheric pressure of 1 atm (Zeebe and Wolf-Gladrow 2001). The partial pressure of water vapour ($H_2O_{(g)}$) in the carrier gas was assumed to be in equilibrium during all experiments, as platinum-cured silicon tubing is highly permeable to water vapour (Andriot et al. 2009). Under the aforementioned assumptions, xCO_2 and pCO_2 are equal, and for simplicity, instrument output will be henceforth denoted as pCO_2. Conditions where xCO_2 and pCO_2 are not equal are discussed in later sections on uncertainty.

A multiple tube housing design for the probe was preferred as this achieved the greatest surface area to volume ratio, making the probe more responsive per unit area (cm^2) and volume (cm^3) than a single or double sided disk design (*see* below). The total volume of the probe including the inlet and outlet tubes was 0.417 cm^3 and the surface area to volume ratio was 69 : 1. Platinum cured silicon tubes were selected for the probe as any alternatives, including expanded- Polytetrafluoroethylene (ePTFE) or Polypropylene (PP) could not be manufactured to a similar specification. In addition, the silicone tubing was extremely flexible and robust which aided assembly and probe handling. Polytetrafluoroethylene (PTFE) tubing was used to carry the gas from the probe to the IRGA as it exhibited a lower CO_2 desorption rate than silicon (Boatman and Lawson unpubl.). The amount of silicon tubing used was minimised because of desorption and consequently only used in a small section to connect the membrane gas exchange unit to the IRGA. PTFE was not suitable due to its reduced flexibility.

An in-house designed integrated computer software programme (CCS) allowed real-time data acquisition of pCO_2, pH, O_2, temperature and salinity, from which the user was able to manipulate and/or regulate pCO_2 and thereby control other linked parameters of the carbonate system. The software libraries used were from National Instruments DAQmx and Microsoft Visual Studio. The CCS computer control was implemented on an Intel Atom Processor Netbook with 1GB system memory; connected to a National Instruments (NI) USB-6009 Data Acquisition (DAQ) board. The DAQ board had eight analogue sensor input channels and eight digital output channels used to manipulate values and pumps to control the system (*see* below). Sensor input (pCO_2/pH_T/O_2), depending on their values (relative to desired pre-set values and thresholds), triggered corresponding response actions to be performed. Each sensor event/response sequence was automatic and deterministic, meaning for every event there was a unique response. Target set-point pCO_2 (pCO_{2sp}) values and tolerance limits for each of these values were set within the software and maintained by the switching of two solenoid valves to: (1) provide ambient air; (2) provide CO_2 free air by running ambient air through a series of soda lime columns to reduced pCO_2; (3) provide pulses (user defined length) of CO_2 from a pure CO_2 gas cylinder to increase pCO_2. A user-defined wait period after each event enabled the system to check whether target values had been reached

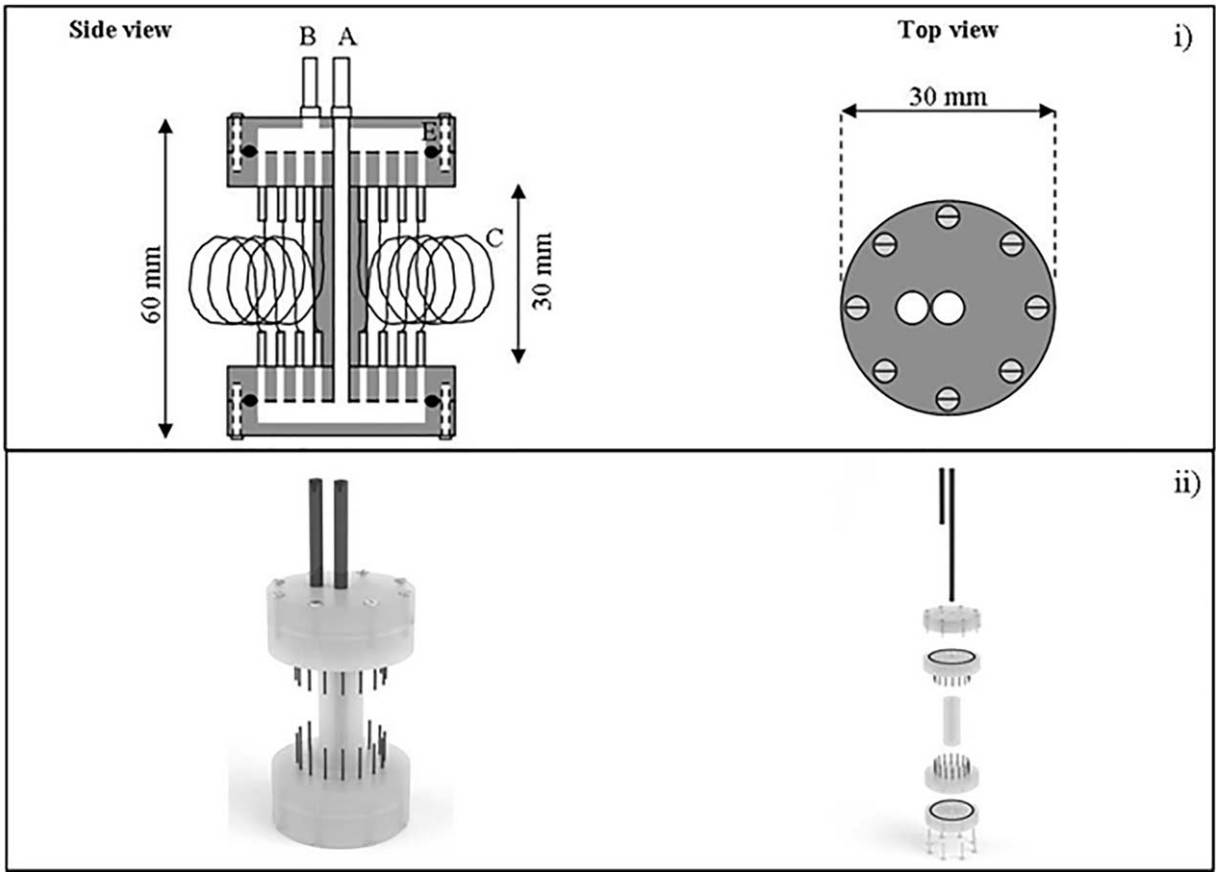

Fig. 2. A schematic (i) and image (ii) of the membrane gas exchange unit. In figure **i)** Air is pumped through a central inlet tube (**A**) and down 18 thin platinum-cured silicone tubes (**C**) (0.31 mm ID, 80 mm in length). The gas stream from the tubes converges at a central air space before leaving the probe through an outlet tube (**B**). The total volume of the probe including the inlet and outlet tubes is 0.417 cm^3. **ii)** A high resolution 3D perspective Cadimage of the Silicone Tube Based Membrane Housing.

before another event was initiated, thus preventing the system driving oscillations in control of the chemistry. The software allowed user defined input of target pCO_{2sp}, pH_T and $[O_2]$, along with sampling rates based on: (1) $pH_{T,}$ (2) $pCO_{2sp,}$ or (3) $[O_2]$ (*see* Supporting Information Fig. 2). Simultaneous real-time measurement of two variables (pH_T and pCO_2) were recorded by the software, from which all interdependent variables of the carbonate chemistry system were calculated using the equilibrium chemical thermodynamic equations and the dissociation constants of Lueker et al. (2000), Dickson (1990) for $KHSO_4$ and Uppström (1974) for borate (Supporting Information Fig. 3).

Calibration of the measurement probes

Instrumentation drifts were minimised by weekly calibrations of pH electrodes and monthly calibration of the IRGAs. The pH probes were calibrated at 25°C using 2-amino-2-hydroxy-1-3-propanediol (TRIS)/Hydrochloric acid (HCl) and 2-aminopyridine (AMP)/HCl buffers in synthetic seawater with a salinity of 35. Buffers were made following CDIAC recommendations (Dickson et al. 2007). The IRGA was zeroed using N_2 gas and the span calibration conducted using 700 (± 2%) ppm xCO_2 in dry air (BOC, UK). The O_2 probe was calibrated using a two point calibration: the first (zero) used media bubbled over night with N_2 gas to remove O_2 gas, and the second calibration point (100%) used media bubbled with ambient air set to 100% after stabilisation. The O_2 calibrations were relative to saturation at ambient temperature and concentration was then calculated based on the equilibrium constants of Benson and Krause (1984). Daily checks of reservoir A_T further confirmed instrument and measurement stability, with A_T verified using certified reference materials distributed by A. Dickson (Scripps Institute of Oceanography).

Testing and optimisation of the system

Tests were performed using artificial seawater (Tropic Marine© PRO REEF salt-based seawater supplemented with $NaHCO_3$) maintained at 25.0 ± 0.9°C and a salinity of 35. To test the stability of the system and the software control, the system was set to a target pCO_{2sp} of 720 μatm and 380 μatm, with a tolerance limit of ± 2 μatm for both tests. The system

monitored every minute for 20 h ($n = 1200$) to assess pCO_2 stability for set-points above and below ambient air pCO_{2atm}. An atmospheric CO_2 level of 720 μatm has been projected as lower or upper bounds within several Intergovernmental Panel on Climate Change (IPCC) scenarios (e.g., RCP 4.5 and RCP 6, IPCC 2014). This value was slightly outside the IRGA calibration window (0–700 ppm), however this exceedance was considered negligible given the strong linearity of the LI-820 from 0 ppm to 1000 ppm xCO_2. Stability tests were constantly bubbled with ambient CO_2, which was periodically switched to CO_2-free or CO_2-enriched air by the control program. The system was open to the atmosphere through a vent tube in the chamber lid (Fig. 2). Tests for stability, temperature sensitivity and response time were conducted under this open system configuration.

Any influence of DIC and temperature on pCO_2 control was also established by running and controlling the system at four temperatures (5°C, 15°C, 25°C, and 35°C) and at three levels of DIC (1.5, 2.0, and 3.5 mmol kg^{-1}) over a range of target pCO_{2sp} between 0 and 1600 μatm. For the temperature comparison, DIC was initially set at 2.0 mmol kg^{-1} by the addition of HCO_3^- and CO_3^{2-} (1 mol L^{-1}) and a salinity of 35. DIC was calculated using CO2SYS (Pierrot and Wallace 2006) from pH_T and A_T. The DIC comparison was conducted at 25°C, and a salinity of 35. Values of pCO_2 measured by the membrane equilibrium system were compared to those derived using variables pH_T and A_T and the equilibrium chemical thermodynamic equations and the dissociation constants of Lueker et al. (2000), Dickson (1990) for $KHSO_4$ and Uppström (1974) for borate.

System response time

To test the response time of the MI-IRGA to changes in dissolved pCO_2, the seawater was bubbled with N_2 to remove pCO_2 and the time taken for pCO_2 measurements to reach a set-target pCO_{2sp} monitored. DIC was initially set to 2.0 mmol kg^{-1} by the addition of HCO_3^- and CO_3^{2-} (1 mol L^{-1}). Five target pCO_{2sp} were set (184, 235, 313, 420 and 518 μatm) and pCO_2 and pH_T measured every minute until target equilibrium was reached. Temperature was maintained at 25.0°C and salinity at 35.

Uncertainty associated with the system

Uncertainty analysis was performed following the method of Dickson 2010 (in Riebesell et al. 2010) to assess the error in estimating A_T and DIC based on pH_T and pCO_2 measurements from the MI-IRGA alone. Uncertainty for each input individually, as well as the combined standard uncertainty (*see* Ellison and Williams 2012), was assessed for all parameters based on an estimation of A_T and DIC. Furthermore, because the method for estimating combined standard uncertainty assumes that each parameter is independent, making it less probably that there will be large errors in multiple input parameters, we also apply a Monte Carlo simulation. In the Monte Carlo simulation, the carbonate parameters of Lueker et al. (2000) were used for K1 and K2, Weiss 1974 for Henry's Law and Fugacity, for KB Dickson (1990), for total Boron Uppström (1974), and a total pH scale with total silicate and pH set to zero. The uncertainties were assessed by generating 10,000 random displacements in the input variables (*see* Table 1). The 95% ellipsoids for maximum possible uncertainty from the variance-covariance matrices were created with maximum likelihood estimate. Measurement uncertainty was determined from the probe and/or instrumentation used to measure the parameter (*see Microcosm design*). The uncertainty associated with K1 and K2 was obtained from Riebesell et al. (2010).

Biological application of the system 1: *Pocillipora damicornis*

We further assessed the capability of the system to measure metabolic drifts under three different light regimes (dark, low-light (130 μmol m^{-2} s^{-1}), and high-light (450 μmol m^{-2} s^{-1}). The microcosms were maintained at 26.0°C using a water bath heated by NeoHeaters (IPX8; Aquael, Poland). Light was supplied cool white LEDS and measured with a 4π spherical underwater quantum sensor (LI–193SA; LI-COR, UK). The microcosms were left under experimental ambient light in an open-configuration for ca. 30 min to reach a stable temperature. A 5 cm fragment of the coral *P. damicornis* was then added and the systems closed and placed under the various light regimes. Corals were originally from the Indo-Pacific and sourced from Tropical Marine Centre Ltd. (Chorleywood, UK). Seawater inside the microcosms were allowed to drift in response to the biological activity of the coral fragment for a further 180 min. Drifts in

Table 1. Monte Carlo input parameters for estimating the uncertainty of calculating A_T and DIC based on the estimated error in the pH and pCO_2 measurements and in the equilibrium constants.

Parameter	Measurement uncertainty	Function (Additive, multiplicative or log)
Salinity	0.1	Additive
Temperature	0.01	Additive
pH_T	0.01	Additive
pCO_2	0.003	Multiplicative
KH	0.01	Log
K1	0.02	Log
K2	0.002	Log
Function	**Equation**	
Additive	Mean + standard deviation * normal distribution(0,1)	
Multiplicative	Mean * (1 + standard deviation * normal distribution(0,1))	
Log	$1\hat{0}$ (mean + standard deviation * normal distribution(0,1))	

pH_T, pCO_2 and $[O_2]$ were monitored continuously over the experimental period to demonstrate the capability of the system to monitor real-time changes in the microcosm environment.

Biological application of the system 2: *Porites cylindrica*

To demonstrate the ability of the system to measure metabolic processes and to assess the sensitivity of the system, we tested for the interactive influence of light, pCO_2 and temperature on photosynthesis, respiration and calcification of the coral species *P. cylindrica*. We repeated the experimentation of Suggett et al. (2013), but instead grew the corals under an elevated temperature of 28.5°C (compared to 26.0°C) to allow for the additional interactive role of growth temperature to be evaluated. Corals were again originally from the Indo-Pacific and sourced from Tropical Marine Centre Ltd. (Chorleywood, UK). Full acclimatisation details follow those described in Suggett et al. (2013). Briefly, 5–8 cm nubbins were acclimatised to two light conditions on a 12 : 12 light : dark cycle: 100 ± 11 and 400 ± 32 μmol photons m^{-2} s^{-1} (150 W Metal-Halide lamp, 14 Kelvin Bulb; Arcadia Products PLC, UK; and measured at the depth of the nubbins with the 4π spherical underwater quantum sensor). After 3 weeks in the acclimatisation tanks, six nubbins from each of the light regimes (high-light, low-light) were placed into separate microcosm vessels under the same conditions as the acclimation tanks; each microcosm was then allowed time to equalise to the desired pCO_2 level. Metabolic drift analysis was subsequently conducted by closing the system and allowing pCO_2, pH_T, $[O_2]$ and A_T to change in response to the coral metabolic activity. A_T was measured (as previously described) at the start and end of the incubation period, while pCO_2, pH_T and $[O_2]$ were continuously measured over the experimental period. Rates of calcification were determined by the alkalinity anomaly technique (Smith and Kinsey 1978) and rates of photosynthesis and respiration by measuring the change in $[O_2]$. All metabolic rates were normalised to coral surface area (cm^{-2}) and thus, calcification (G), photosynthesis (P) and respiration (R) were in units of μmol $CaCO_3$ cm^{-2} h^{-1} and O_2 cm^{-2} h^{-1} respectively.

$$G = \left[\frac{(\Delta AT \cdot \rho \cdot 0.5) \cdot V}{I_t \cdot SA}\right] \quad (1)$$

where ΔAT = describes the change in total alkalinity (μmol L^{-1}), V = volume of seawater (L) within the microcosm, I_t (h) is incubation time, SA is the coral surface area (cm^{-2}), ρ is the density of seawater and 0.5 accounts for the decrease of A_T by two equivalents for each mole of $CaCO_3$ precipitated.

$$P \text{ and } R = \left[\frac{(\Delta O_2) \cdot V}{I_t \cdot SA}\right] \quad (2)$$

where ΔO_2 = describes the change of O_2 and rates normalised as described for calcification (Eq. 1).

Field application of the system

To further evaluate how well pCO_2 was retrieved by the MI-IRGA for a natural system, we additionally tested the unit at a field location in Little Cayman, Cayman Islands, British West Indies, during June 2014. Results from the unit were compared to pCO_2 derived from parallel measurements of pH_T and A_T. Over three 24 h periods, discrete water samples were collected from a seagrass dominated lagoon, where high photoautotroph biomass creates large diel fluctuations in pCO_2 (*see* Camp et al. 2016b), thereby testing the sensitivity range of the unit. Sampling was conducted every 3 h over a 72 h period ($n = 24$). Water samples were collected and stored as recommended under CDIAC protocols (Dickson et al. 2007). At the time of water collection, in situ temperature, conductivity and pH_T were measured using the ORION 5 Star meter (Model A329; Fisher Scientific, U.S.A.) with a pH_T/temperature probe (combination probe Ross Ultra*; Fisher Scientific*, U.S.A., accuracy and precision of 0.01 pH units), and conductivity probe (ORION Duraprobe 4-Electrode Conductivity cell, Model 013005A; Fisher Scientific, U.S.A.). In situ conditions and pH_T and A_T were then used to calculate pCO_2. A_T was measured as previously described using the Titrino titrator (Model 848; Metrohm, UK). In addition, each water sample was processed in the microcosm chamber for 60 min to directly measure pCO_2.

Statistical analysis

To assess whether the computer software and control system were best able to maintain low or high pCO_2 levels, the deviation from the target high and low pCO_{2sp} values were compared via an independent sample t-test. Parametric test assumptions were met, as demonstrated by the Bartlett test for homogeneity of variance and qq-plots for normality. The response time of the MI-IRGA system to dissolved pCO_2 in seawater for the five pCO_2 readings was analysed using a regression, as was the derived pCO_2 to measured pCO_2 values for the field experimentation, and also the systems performance across temperatures and DIC levels. Linear Mixed Effects (LME) models were applied, with experimental time as a random effect, to examine the effect of temperature, pCO_2 and light on calcification, respiration and photosynthesis. Cleveland dot-plots were used to determine outliers and boxplots and scatterplots were used to check for co-linearity within the dataset (Zuur et al. 2010). Assumptions of linearity, independence, homoscedasticity and normality were met. The model was fitted using the lme function in the nlme package in R software (R Development Core Team 2011). Model simplification was undertaken using analysis of variance (ANOVA) to compare models with progressively simplified fixed effects, thus ensuring correct p values (Crawley 2007). Acceptability of the model was tested by plotting the residuals against: (1) fitted values to check for homogeneity and (2) each explanatory variable in the model

to check for violations of independence (Zuur et al. 2010). Parameter estimation in LME models was done based on Restricted Maximum Likelihood (REML). All statistical analysis were conducted in R (R Development Core Team 2011) and SigmaPlot® 10.0.

Results

Testing and optimisation

The MI-IRGA system maintained an average pCO_2 of 382 ± 1 μatm and 722 ± 4 μatm over 20 h tests for set-points of 380 and 720 μatm, respectively (Fig. 3). In both cases, average pCO_2 was ca. 2 μatm higher than the set-point despite opposite air-water gradients. Potential explanations for this positive deviation are discussed in the following section. We expect that the two minima in Fig. 3A are due to a decrease in ambient pCO_2 below 380 μatm. Only the minima recorded at 230 min exceeded the tolerance threshold and triggered injection of CO_2-enriched air. CO_2-free air was unnecessary for the 720 μatm set-point, as the chamber was continuously bubbled with ambient air. It should be noted that the slope and duration of the pCO_2 spikes after injection of pCO_2-enriched air (Fig. 3B) varied throughout the 20 h test interval. This variability was presumably associated with retention of CO_2-enriched bubbles at the water surface. Furthermore, the MI-IRGA system sustained pCO_2 measurements in seawater over the range of temperatures (5–35°C, Fig. 4A) and DIC (1.5–3.5 mmol kg^{-1}, Fig. 4B) tested, with an approximate 1 : 1 ratio achieved between the measured vs. derived pCO_2 (temperature: slope = 0.97 ± 0.01, $r^2 = 0.99$, $n = 71$, $p < 0.001$; DIC: slope = 0.98 ± 0.01 $r^2 = 0.99$, $n = 55$, $p < 0.001$).

Response time

Time taken for the MI-RGA system to re-equilibrate from zero pCO_2 to a range of target pCO_{2sp} values between 184 and 518 μatm, was 18–23 min (Fig. 5A). In spite of the different ranges in equilibration concentrations, a linear relationship was observed between re-equilibration time and (new) target pCO_{2sp}; this likely reflects the expected proportionate change in the difference between target and initial pCO_2 with equilibration time. Considering a naturally expected change in pCO_2, i.e., of 5–10% within a reef setting (Kayanne et al. 2005), the significantly linear relationship between these two measurements ($r^2 = 0.78$, $n = 5$, $p < 0.01$; Fig. 5B) yielded an overall system equilibration time of ca.12 μatm min^{-1} to reach a target pCO_2 518 μatm from a starting ambient of 380 μatm. The system response time (τ), quantified here as the time required to reach 63.2% of the change in pCO_2, ranged from about 4–6 min (Fig. 5B).

Biological application 1: *Pocillipora damicronis*

The system detected real-time biologically induced changes in the pH_T, pCO_2 and $[O_2]$ within the microcosm environment as a result of the *P. damicornis* metabolic activity. Both high- and low-light resulted in $[O_2]$ increasing by 0.6 and 0.1 μM per min^{-1}, respectively (Fig. 6A,B). However, under low-light, pCO_2 increased by 0.1 μatm per min^{-1} and pH_T decreased by 0.0008 units per min^{-1}, vs. high-light where pCO_2 decreased by 0.4 μatm per min^{-1} and pH_T increased by 0.0007 units per min^{-1}. Differences between rates of carbon fixation and calcification between the two light-regimes likely account for the physiological response measured. Under darkness, pCO_2 increased by 1.6 μatm per min^{-1}, while both pH_T and $[O_2]$ decreased by 0.0014 units and 0.2 μatm per min^{-1}, respectively (Fig. 6C); thus demonstrating respiration in the absence of photosynthesis. This initial biological application demonstrates how the system can be used to determine rates of change, and their trajectory in relation to each other, in real-time.

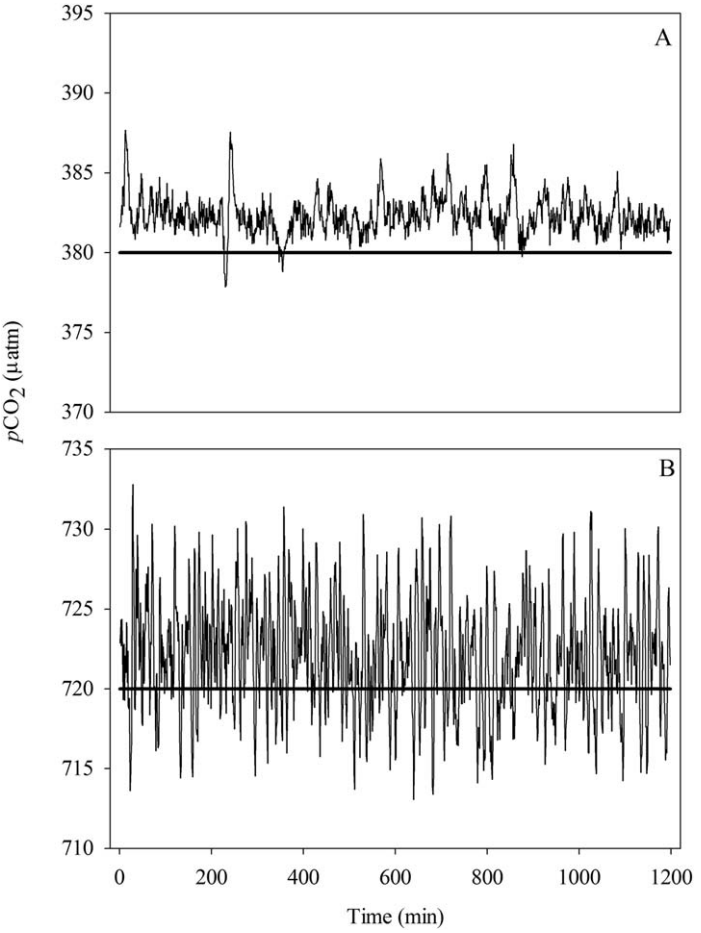

Fig. 3. Stability of the system at maintaining desired set-point pCO_{2sp} values over a 20 h period. The CCS software and control system were able to maintain two desired pCO_{2sp} values (black horizontal lines: 380 and 720 μatm) within (mean ± standard error, $n = 1200$) 2.2 ± 0.07 μatm over a 20 h period. Over the 20 h period the maximum deviation from the desired levels was 12.8 μatm, with slightly more deviation at the higher (720 μatm) target value ($t = -2.762$, df = 1200, $p < 0.01$).

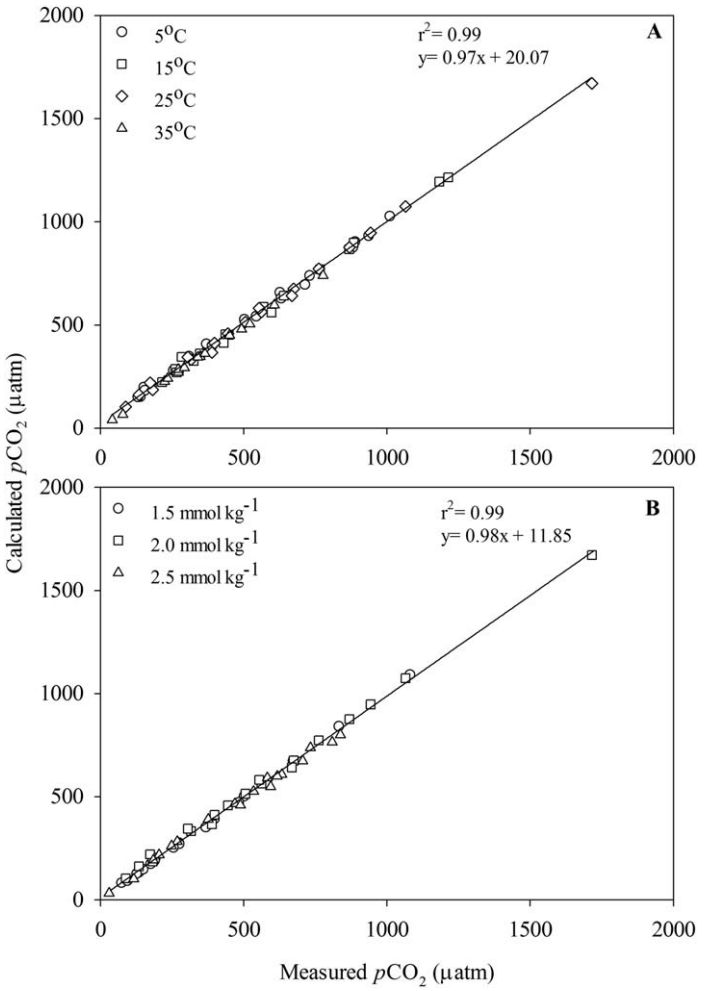

Fig. 4. A comparison of measured and calculated pCO_2 at: (**A**) four temperatures and, (**B**) three levels of DIC, over the range of 0–1600 μatm of CO_2 in seawater. Temperature comparisons were conducted at 2.0 mmol kg^{-1} DIC, while DIC comparisons were maintained at 25°C. Both comparisons resulted in a 1 : 1 ratio between measured and calculated pCO_2.

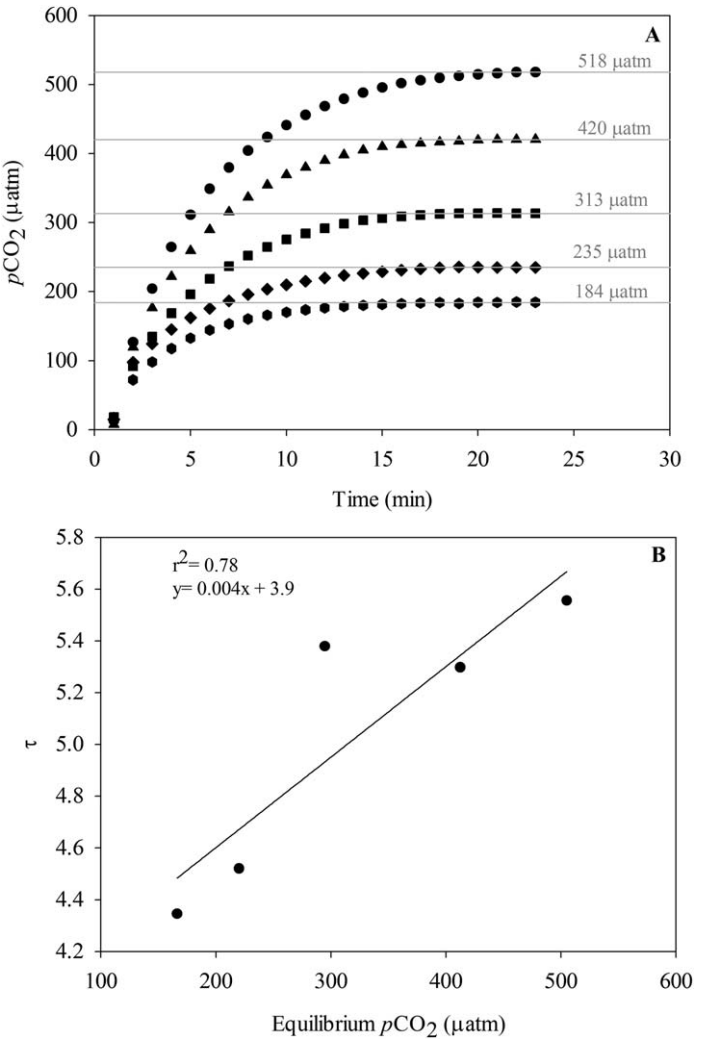

Fig. 5. The equilibrium time of the system between pCO_{2atm} in air and pCO_2 in water for five pCO_2 target levels. Temperature was maintained at 26 ± 0.9°C and salinity at 35. (**A**) Response time of the system per target $pCO_{2sp.}$ Target values are indicated by the solid black horizontal lines. (**B**) System response time (τ) to step changes in pCO_2. From zero pCO_2 the system took between 18 and 23 min to reach equilibrium between pCO_{2atm} in air phase and pCO_2 in water phase; however, the significantly linear relationship between equilibrium time and equilibrium pCO_2 enabled a system response time of ca.12 μatm min^{-1} to be determined from an ambient pCO_{2atm} level of 380 μatm to reach a higher target pCO_{2sp}.

Biological application 2: *Porites cylindrica*

Calcification rates obtained from the metabolic A_T drifts were nearly four times higher under high-light (0.34 ± 0.03 μmol $CaCO_3$ cm^{-2} h^{-1}) than at low-light (0.09 ± 0.01 μmol $CaCO_3$ cm^{-2} h^{-1}) ($t = 2.686$, $p < 0.05$; Fig. 7; Table 2), with the high-light treatment sustaining greater levels (ca. 8 times higher) of calcification under elevated pCO_2 ($t = 3.013$, $p < 0.01$; Fig. 7; Table 2). Temperature alone did not influence rates of calcification, however it showed an interactive effect with light resulting in elevated (2.3 times greater) calcification under the high-temperature, high-light treatment (*see* Fig. 7; Table 2). All three parameters also had an interactive effect on calcification (*see* Table 2). Rates of photosynthesis were elevated under the high-light treatments as per calcification; however no other interactions were observed. Respiration rates showed no significant variability across experimental treatments despite the elevated levels under the high-light treatments (*see* Fig. 7).

Field application of the system

The MI-IRGA system used at the field site was capable of measuring the full diurnal range of seawater pCO_2 (ca.130–540 μatm) (Fig. 8). Measured and derived pCO_2 values followed the same daily trajectories, but with the measured values of pCO_2 consistently higher (by a mean ± standard error value of 5.5 ± 0.4 μatm) than the calculated values.

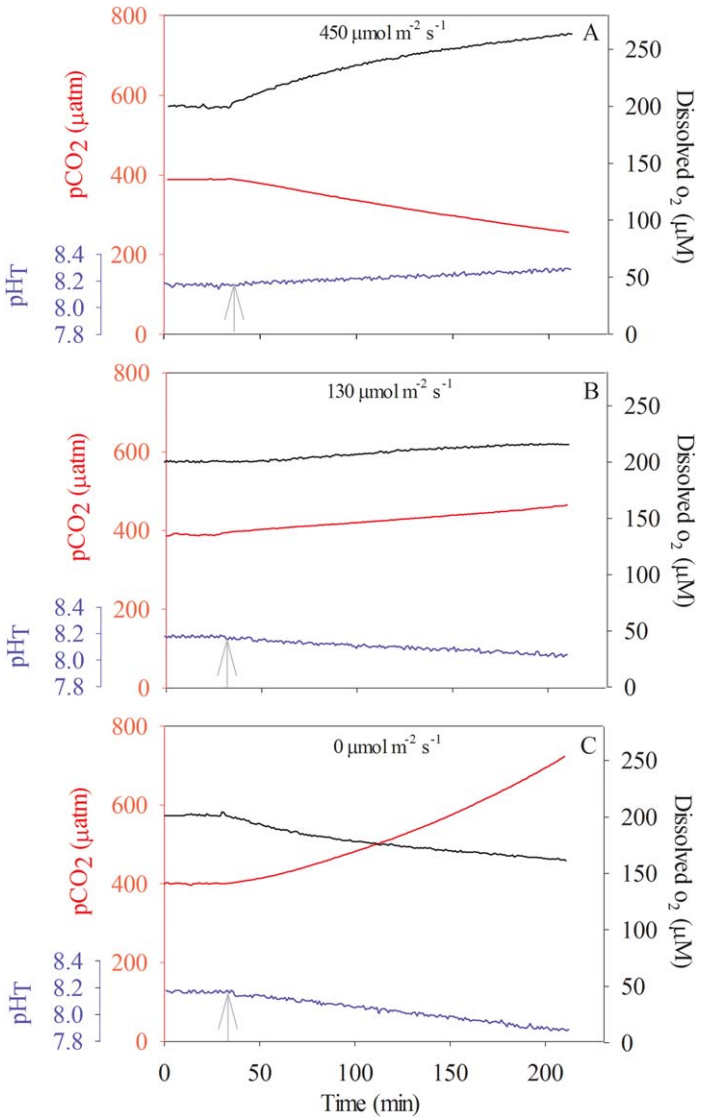

Fig. 6. An example of the continuous pH_T, pCO_2 and O_2 measurements achieved in the microcosm using *Pocillipora damicornis* as a study organism. Microcosms were held at open-steady-state conditions for ca. 30 min before a 5 cm fragment of *P. damicornis* was added, the system closed (as indicated by the grey arrow) and placed under: (**A**) high (450 μM m^{-2} s^{-1}), (**B**) low (130 μM m^{-2} s^{-1}) or (**C**) dark light conditions. Drifts in pH_T, pCO_2 and O_2 were continuously measured for 180 min.

Derived and measured pCO_2 values were strongly correlated ($r = 0.999$, $n = 24$, $p < 0.001$) demonstrating the field capability for the MI-IRGA to return in situ pCO_2 in real-time in a manner that is consistent with established methods, based on discrete semi-continuous sampling for pH_T and A_T.

Discussion

Our novel MI-IRGA system provides real-time continuous measurement of pH_T, pCO_2, temperature and salinity, which allows immediate estimation of the full carbonate chemistry system, and thus real-time user control over the microcosm system. Combined with [O_2] measurements, the system also allows analysis of the physiological response of benthic and pelagic phototrophs. We demonstrate the application of the system for individual taxa, but the system could conceivably be scaled to accommodate larger organisms and/or mixed community ecological-scale assessment and experimentation.

Control performance

The system response time is the most significant factor determining the overall performance of the MI-IRGA system in measuring and controlling pCO_2.

At 26.0°C, the time constant for the system response to a change in the pCO_2 of the bubbled air was approximately 5 min (Fig. 5). Thus, a delay of at least 5 min is advisable between pulses of CO_2-free or CO_2-enriched air to prevent over-adjustment. The pCO_2 control performance also depends on the absolute difference between pCO_2 in the ambient air (pCO_{2atm}), the control gas (pCO_{2ctr}) and the set-point (pCO_{2sp}). When pCO_{2sp} - pCO_{2atm} is small, the system requires infrequent adjustment to correct for air-water gas exchange. If pCO_{2sp} - pCO_{2ctr} is also small, then the MI-IRGA will maintain a stable pCO_2 near the tolerance point closest to pCO_{2atm}, as observed during the 380 μatm stability test (Fig. 3A). When pCO_{2sp} - pCO_{2atm} is large, frequent pulses of pCO_{2ctr} are required, as occurred during the 720 μatm stability test (Fig. 3B). If pCO_{2sp} - pCO_{2ctr} is also large, the mean and variation of the water pCO_2 will depend on the counteracting gas exchange rates for the two gasses being bubbled. The large difference between pCO_{2sp} and pCO_{2ctr} during the 720 μatm stability test led to higher variability and shifted the mean pCO_2 toward pCO_{2ctr} rather than pCO_{2atm}. Performance may therefore be increased by reducing pCO_{2sp} - pCO_{2ctr} and increasing pulse duration of CO_2-enriched air.

The response time of the probe to a change in water pCO_2 is determined by the surface area of membrane available for diffusion, the diffusion rate across the membrane and the flow rate and volume of the recirculation gas. Our current configuration enabled an equilibration time of ca. 20 min and a response time constant of ca. 5 min. Thus absolute values of pCO_2 cannot be determined for shifts that occur at time scales less than 20 min, but relative changes in pCO_2 can be detected relatively quickly. In normal marine scenarios pCO_2 can change on the order of 0.19 μatm min^{-1} on highly dynamic reef flats (Albright et al. 2013) with open-ocean changes being even slower (Guadayol et al. 2014); thus, our response times would be capable of capturing natural variability in marine systems.

Measurement uncertainty

Cross-sensitivity of xCO_2 and $H_2O_{(g)}$ is the largest sources of uncertainty in the MI-IRGA pCO_2 output; the LI-820

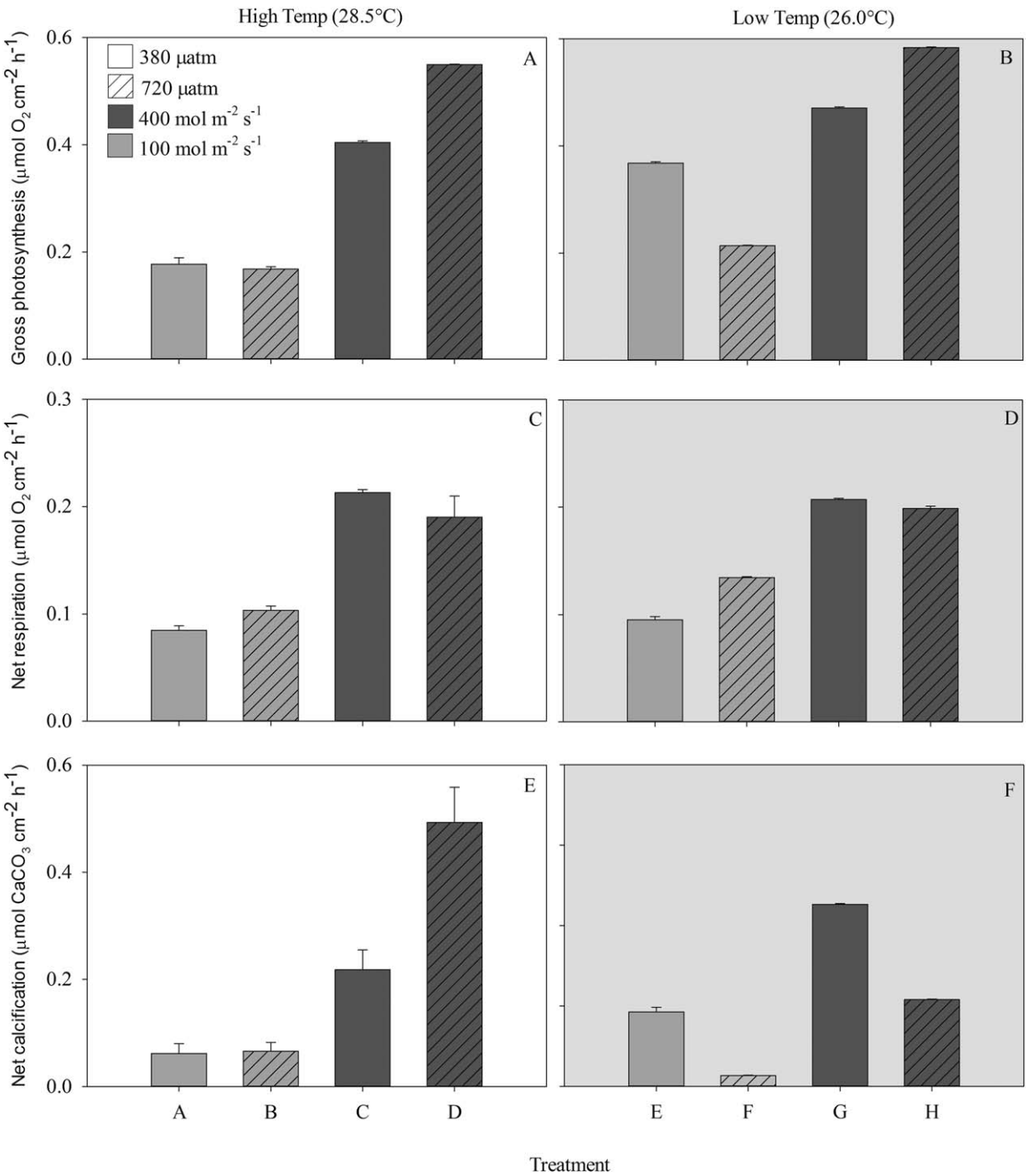

Fig. 7. Physiological measurements for *Porites cylindrica* exposed to high and low temperature, light and pCO_2. Corals were exposed to high (28.5°C) or low (26°C) temperature, high (400 μmol m^{-2} s^{-1}) or low (100 μmol m^{-2} s^{-1}) light and/or high (720 μatm) or low (320 μatm) CO_2 levels. Treatments (**A**), (**C**), and (**E**) were at high-temperature and (**B**), (**D**) and (**F**) were at low-temperature. Output of statistical analysis are shown in Table 2.

measurement accuracy decreases from $< 0.5\%$ of the xCO_2 reading in dry air to $< 1.5\%$ of the xCO_2 reading in humidified air. However, a humidified carrier gas reduces the correction needed to account for the $pH_2O_{(g)}$ when xCO_2 is measured in dry air. At 26.0°C and a salinity of 35, xCO_2 in dry air is about 3.5% higher than water pCO_2 (Weiss and Price 1980). Here we assumed that $pH_2O_{(g)}$ in the carrier gas was at equilibrium with water pH_2O, but even if $pH_2O_{(g)}$ was

Table 2. Linear Mixed Effect (LME) model parameters for calcification, respiration and photosynthesis with experimental time modelled as a random effect.

Model terms	Estimate	SE	*t*-value	*p*-value
Intercept: calcification				
Light	0.015	0.006	2.686	0.01
pCO_2	−0.002	0.003	−0.549	N/S
Temperature	−0.024	0.089	−0.274	N/S
Light: pCO_2	−0.001	0.001	−3.013	0.01
Light:Temperature	−0.001	0.001	−2.559	0.01
pCO_2:Temperature	−0.001	0.001	0.425	N/S
Light: pCO_2:Temperature	0.001	0.001	3.038	0.01
Intercept: photosynthesis				
Light	−0.021	0.010	−2.145	0.05
pCO_2	−0.006	0.005	−1.170	N/S
Temperature	−0.300	0.105	−2.843	0.05
Light: pCO_2	0.001	0.001	1.461	N/S
Light:Temperature	0.001	0.001	2.065	0.05
pCO_2:Temperature	0.001	0.001	1.097	N/S
Light: pCO_2:Temperature	−0.001	0.001	−1.347	N/S
Intercept: respiration				
Light	−0.005	0.003	−1.447	N/S
pCO_2	−0.001	0.002	−0.510	N/S
Temperature	−0.063	0.034	−1.847	N/S
Light: pCO_2	0.001	0.001	0.333	N/S
Light:Temperature	0.001	0.001	1.542	N/S
pCO_2:Temperature	0.001	0.001	0.536	N/S
Light: pCO_2:Temperature	−0.001	0.001	−0.378	N/S

Significance is shown at 95% and N/S indicates a non-significant result.

slightly below air-water equilibrium, the effect on the xCO_2 reading would be partially offset by the decrease in IRGA cross sensitivity. Small variations in ambient atmospheric pressure also contribute to pCO_2 uncertainty, but these variations are typically < 1%. Because ambient atmospheric pressure and $H_2O_{(g)}$ were not measured in this study, we adopt a conservative uncertainty estimate of ± 3% of the pCO_2 reading. However, this uncertainty could be reduced to as low as 0.5% in future application by measuring pressure and $H_2O_{(g)}$. These estimates exclude the uncertainty associated with calibration gas, as this will depend on the purity and calibration method used.

Calculation uncertainty

The control programme calculated and displayed carbonate system parameters in real-time based on continuous pCO_2 and pH_T measurements and user-defined thermodynamic equilibrium constants of the carbonate system. The uncertainty associated with each input individually and the combined standard uncertainty of all parameters in estimating A_T and DIC are shown in Table 3 (following Dickson 2010, in Riebesell et al. 2010). The method for estimating

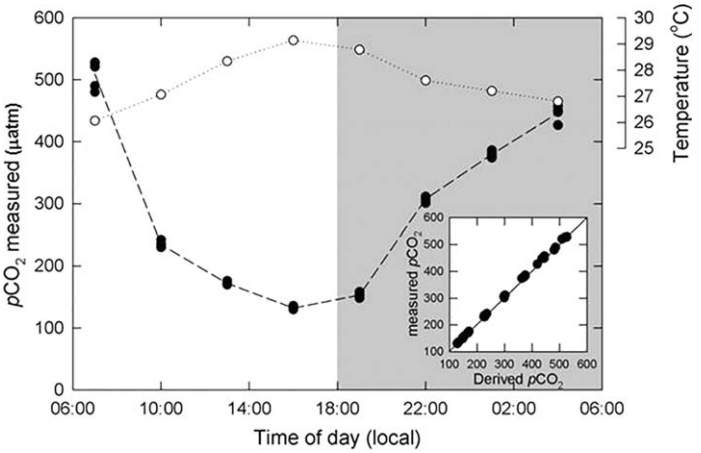

Fig. 8. The in situ diurnal pCO_2 and temperature trend for a seagrass site in Little Cayman, Cayman Islands, British West Indies, with a comparison to derived pCO_2 values. Discrete water samples were collected every 3 h (eight time point per day) over a 3 d period in June 2014 ($n = 24$), with all data presented. For each sample, (i) pCO_2 was directly measured within the laboratory and (ii) pCO_2 was derived from in situ temperature, salinity, depth as a proxy for pressure, pH_T and A_T. Values of derived and measured pCO_2 demonstrated high co-variability ($r = 0.999$, $n = 24$, $p < 0.01$).

combined standard uncertainty (Ellison and Williams 2012) assumes that each parameter is independent, which makes it less probable that there will be large errors in multiple input parameters. However, it is likely that uncertainty is higher, as many of the input parameters are correlated, particularly the equilibrium constants. Uncertainty could be as high as 15% if we consider the contribution from each parameter to be cumulative, but even this estimate assumes that the correlation is linear. Figure 9 shows how uncertainty from the MI-IRGA measurement error exacerbates uncertainty in the carbonate chemistry equilibrium equations. Some uncertainty could be reduced by improving the accuracy of calibration standards and sensors; for example, measuring $H_2O_{(g)}$ in the recirculation loop would reduce pCO_2 uncertainty by about 50%, and the use of high accuracy pH probes would reduce measurement error from 0.01 to 0.001. The pCO_2-pH_T pair yields the highest uncertainty when calculating the remaining carbonate system parameters as reflected in the Monte Carlo simulation as an ellipse around the estimated DIC and A_T concentrations (Fig. 9). The diagonal ellipse shows that there is disproportionately large uncertainty when A_T and DIC are changing simultaneously, as would occur due to calcification/dissolution. However, the uncertainty is much lower if only the DIC is changing, as would occur due to photosynthesis/respiration and therefore the system is well suited for conditions where production/respiration are the dominant controls on carbonate chemistry (Table 3; Fig. 9). Our uncertainty structure indicates that estimating A_T and DIC by the MI-IRGA would require a direct-point measurement of A_T (as performed in the studies presented here) to

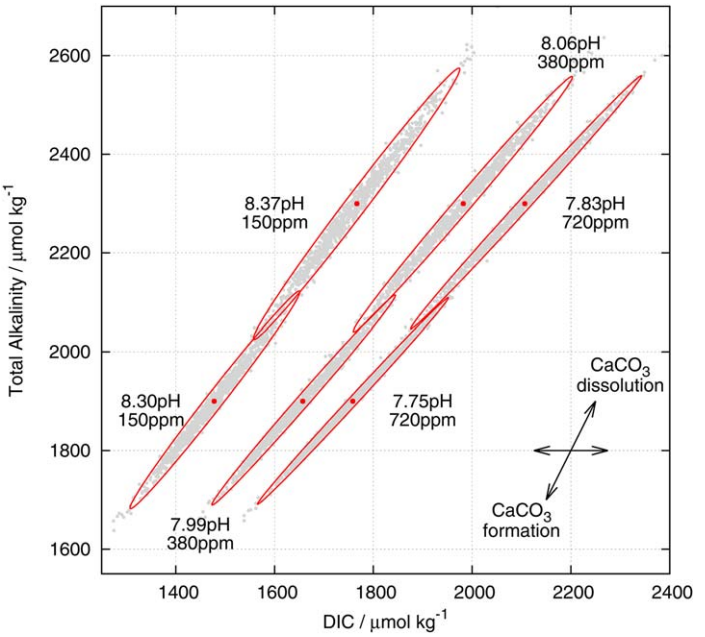

Fig. 9. Monte Carlo simulation to assess the uncertainty of calculating A_T and DIC based on the estimated error in the pH_T and pCO_2 measurements and in the equilibrium constants. The carbonate parameters of Lueker et al. (2000) were used for K1 and K2, Weiss 1974 for Henry's Law and Fugacity, for KB Dickson (1990), for total Boron Uppström (1974), and a total pH scale with total silicate and pH set to zero. The uncertainties were assessed by generating 10,000 random displacements in the input variables (*see* Table 1). The 95% confidence ellipsoids calculated from the variance-covariance matrices (maximum likelihood estimate).

calculate calcification rates due to the error associated with these determinations.

Application

The novel microcosm system described here continuously measures two carbonate chemistry parameters (pH_T and pCO_2) in real-time, and coupled with the in-house designed CCS software allows real-time calculation of all components of the DIC pool. Recent work by Comeau et al. (2014) and Jokiel (2013) demonstrated that control of all DIC parameters are necessary to resolve different species-specific responses in ocean acidification experimentations. HCO_3^- for example can be used by certain taxa to mitigate some of the negative effects of declining calcification under ocean acidification (Comeau et al. 2014). Similarly, the work of Bach et al. (2013) demonstrated that the level to which the calcification rates of *Emiliania huxleyi* are influenced is dependent on which component of the DIC is altered. This only adds to the complexities and difficulties in predicting the responses of communities and ecosystems to ocean acidification and highlights the necessity of a system such as the MI-IRGA.

Table 3. The uncertainty associated with each input individually and the combined standard uncertainty of all parameters in estimating A_T and DIC as described by Dickson 2010 (in Riebesell et al. 2010).

			Calculation uncertainty	
Parameter	Value	Measurement error	DIC*	A_T*
Temperature (°C)	26	0.1	<0.1%	<0.1%
pH_T	7.8, 8.0	0.1	2.6%	2.6%
pCO_2 (μatm)	380, 720	3%	2.9%	2.9%
Salinity	35	0.5	0.4%	0.4%
CO_2 std (μatm)	700	2%	2.0%	1.5%
pK1	5.84	0.01†	4.1%	4.2%
pK2	9.36	0.02†	2.9%	3.3%
Combined standard uncertainty			4.8%	4.8%

*Average values from uncertainty quantification at high and low uncertainty for both 380 and 720.
†From Dickson 2010 in Riebesell et al. (2010).
pK values are from Lueker et al. (2000).

The capability of the MI-IRGA to control pCO_2 in small vessels make it well suited for ocean acidification experiments where replication across multiple treatments is necessary. The system can also be used for culture experiments and is a practical alternative to a membrane contactor gas exchanger. The membrane contactor gas exchanger requires water filtration for dense cultures and in experiments where this is not possible, the system we described can be used. The high-resolution measurements of pCO_2 and pH_T make the MI-IRGA a useful tool to quantify net metabolism based on relative changes in dissolved O_2, pCO_2, and pH_T (e.g., Fig. 6). If additional A_T samples are taken during a closed-system experiment (as per our described methods), the continuous pH_T and pCO_2 data recorded by the MI-IRGA would help resolve how calcification changes over time (e.g., Fig. 7). The large uncertainty in calculating A_T based only on pH_T and pCO_2 measurements, restricts the MI-IRGA for estimating absolute constraints of the carbonate system, for example estimating aragonite and calcite saturation states.

We used the system to explore a previously undescribed interaction of light, temperature and pCO_2 on the coral *P. cylindrica*. Suggett et al. (2013) recently showed for this species that high-light could dampen the negative impact of elevated CO_2 on light calcification. Our data expands on the results of Suggett et al. (2013), finding the same response under high-light, but importantly, that elevated temperature can further enhance calcification. Ocean acidification/temperature experiments have shown that a moderate increase in temperature can enhance calcification (Reynaud et al. 2003), however, that thermal windows are tightly governed and species-specific (Coles and Jokiel 1978). Together, these

data provide examples of how the system can be used to experimentally examine (control for) the impact of changing climatic conditions on influencing key metabolic processes, as well as monitor system carbon chemistry (and hence any role of ecosystem metabolism) needed to resolve how different habitats operate as sources or sinks of atmospheric CO_2. Our thorough assessment of the system and the continuing development of new technologies, and increased specificity of instrumentation, means that improvement to such a system are, and will be, possible in the future. Below we have outlined some recommendations that could be made on future instrumentation development.

Comments and recommendations

In developing the MI-IRGA, we initially tested different system materials for the membrane gas exchanger unit (*see* "Materials and procedures"); however, there are other aspects of the system that could be further developed to improve the sensitivity and resolution of the system. Key areas for future development are:

i. Design features: Increasing the number of tubes would increase the surface area to volume ratio and could decrease equilibration times. A multiple disk design could also potentially be used to hold the membrane of different materials rather than silicon, or PTFE tubes; such an approach may be beneficial for long-term culture studies where biofouling may become an issue. The advantage of using a double (or single) sided membrane probe is that the membrane itself can be routinely and easily cleaned using synthetic swabs. An additional advantage is the range of membrane materials that could be utilised in a disk housing design, for example PTFE membrane (which has comparatively faster diffusion and response rates), and the rigid nature allows it to function under higher pressures (Gibson et al. 1998) which may be beneficial in the field where physical regimes may be highly variable. However, the disadvantage of employing a disk housing design is the comparatively large gas stream volumes required, and therefore these types would only be beneficial in experimental setups or microcosms larger than the one described here.
ii. Improve accuracy of resolving the entire DIC pool by reducing the need to calibrate existing pH probes and/or using new pH probe technologies that have been developed (e.g., Non-invasive pH sensors; PreSens, Germany). In addition, the system could intermittently measure ambient pCO_{2atm} to assist in pCO_{2sp} control.
iii. Improved delivery of air/CO_2 into the system for controlling carbonate chemistry by reduced the bubble sizes. This would increase the frequency with which the chemistry of the system can be resolved and would reduce the time taken to reach a new steady state [CO_2] (*see* Tamburic et al. 2015).
iv. We provide conservation assumptions in our assessment, e.g., assuming the partial pressure of water vapour in the carrier gas to be in equilibrium during all experiments. Water vapour is influenced by temperature and the effect is therefore non-linear. A correction could therefore be incorporated into the software to account for the water vapour effect. This would improve the accuracy of the direct pCO_2 measurement and reduce uncertainty associated with the carbonate system calculations.
v. Incorporation of a miniature waterproof IRGA (*see* Bastviken et al. 2015) that could be situated inside the vessel or on the lid. This would reduce the length of tubing from the exchanger to the IRGA, facilitating quicker equilibrium times. Similarly, enhanced ruggedisation of the system to ensure full field deployability.

Conclusions

Here, we have described and demonstrated the performance of a novel pCO_2 membrane equilibrium system that allows real-time control and monitoring of pCO_2. Coupled with continuous measurements of pH_T and O_2 the system allows real-time monitoring of metabolic processes within the microcosm. Future ocean acidification research needs to recognise the variable response of species to the whole carbonate system and the need therefore for full DIC and metabolic real-time calculation and optional user-control, which the system described here allows. We have extensively validated the system in the laboratory across a range of temperatures, DIC and pCO_2 levels. Using this system we have been able to demonstrate the interactive effect of light, temperature and pCO_2 on the physiology of the coral *P. cylindrica*. High-light dampened the negative influence of pCO_2 on calcification and suggests that increased temperature may enhance calcification rates in some species. The instrument can be used for a range of benthic and pelagic organisms, in both field and laboratory environments. The system is able to measure the diurnal range of conditions experienced within natural systems. As tested, our system constrains fluctuations to well within those experienced by corals in shallow coastal systems where pH is particularly variable. However, we outline a number of improvements that will further enable the system to become scalable to broader applications, across marine biota and ecosystems.

References

Albright, R., C. Langdon, and K. R. N. Anthony. 2013. Dynamics of seawater carbonate chemistry, productivity and calcification of a coral reef flat, central Great Barrier Reef. Biogeosciences **10**: 6747–6758. doi:10.5194/bg-10-6747-2013

Andriot, M., and others. 2009. Silicones in industrial applications. *In* Silicon-based inorganic polymers. V. 84.

Anthony, K. R. N., D. I. Kline, G. Diaz-Pulido, S. Dove, and O. Hoegh-Guldberg. 2008. Ocean acidification causes bleaching and productivity loss in coral reef builders. Proc. Natl. Acad. Sci. USA **105**: 17442–17446. doi:10.1073/pnas.0804478105

Bach, L. T., and others. 2013. Dissecting the impact of CO_2 and pH on the mechanisms of photosynthesis and calcification in the coccolithophore *Emiliania huxleyi*. New Phytol. **199**: 121–134. doi:10.1111/nph.12225

Bastviken, D., I. Sundgren, S. Natchimuthu, H. Reyier, and M. Gålfalk. 2015. Technical note: Cost-efficient approaches to measure carbon dioxide (CO_2) fluxes and concentrations in terrestrial and aquatic environments using mini loggers. Biogeosciences **12**: 2357–2380. doi:10.5194/bgd-12-2357-2015

Benson, B. B., and D. Krause. 1984. The concentration and isotopic fractionation of oxygen dissolved in freshwater and seawater in equilibrium with the atmosphere. Limnol. Oceanogr. **29**: 620–632. doi:10.4319/lo.1984.29.3.0620

Bockmon, E., E. Frieder, C. A. Navarro, L. A. White-Kershek, and A. G. Dickson. 2013. Technical note: Controlled experimental aquarium system for multi-stressor investigation of carbonate chemistry, oxygen saturation, and temperature. Biogeosciences **10**: 5967–5975. doi:10.5194/bg-10-5967-2013

Brading, P., M. E. Warner, P. Davey, D. J. Smith, E. P. Achterberg, and D. J. Suggett. 2011. Differential effects of ocean acidification on growth and photosynthesis among phylotypes of Symbiodinium (Dinophyceae). Limnol. Oceanogr. **56**: 927–938. doi:10.4319/lo.2011.56.3.0927

Byrne, R., and others. 2010. Sensors and Systems for In Situ Observations of Marine Carbon Dioxide System Variables in *Proceedings of OceanObs'09: Sustained Ocean Observations and Information for Society (Vol. 2),* Venice, Italy, 21–25 September 2009, Hall, J., Harrison, D.E. & Stammer, D., Eds., ESA Publication WPP-306, doi:10.5270/OceanObs09.cwp.13

Camp, E. F., D. J. Smith, C. Evenhuis, I. Enochs, D. Manzello, S. Woodcock, and D. J. Suggett. 2016a. Acclimatization to high-variance habitats does not enhance physiological tolerance of two key Caribbean corals to future temperature and pH. Proc. R. Soc. London B. **283**: 1831. doi:10.1098/rspb.2016.0442

Camp, E. F., D. J. Suggett, G. Gendron, J. Jompa, C. M. Manfrino, and D. J. Smith. 2016b. Mangrove and Seagrass Beds Provide Different Biogeochemical Services for Corals Threatened by Climate Change. Front. Mar. Sci. **5**: 52. http://dx.doi.org/10.3389/fmars.2016.00052

Campbell, J. E., and J. W. Fourqurean. 2011. Novel methodology for in situ carbon dioxide enrichment of benthic ecosystems. Limnol. Oceanogr.: Methods **9**: 97–109. doi:10.4319/lom.2011.9.97

Coelho, F. J. R. C., and others. 2013. Development and validation of an experimental life support system for assessing the effects of global climate change and environmental contamination on estuarine and coastal marine benthic communities. Glob. Change Biol. **19**: 2584–2595. doi:10.1111/gcb.12227

Coles, S. L., and P. L. Jokiel. 1978. Synergistic effects of temperature, salinity and light on the hermatypic coral *Montipora verrucosa*. Mar. Biol. **49**: 187–195. doi:10.1007/BF00391130

Collins, S., and G. Bell. 2004. Phenotypic consequences of 1,000 generations of selection at elevated CO_2 in a green alga. Nature **431**: 566–569. doi:10.1038/nature02945

Comeau, S., R. C. Carpenter, and P. J. Edmunds. 2014. Coral reef calcifiers buffer their response to ocean acidification using both bicarbonate and carbonate. Proc. R. Soc. B. **280**: 201223. doi:10.1098/rspb.2012.2374

Crawley, M. 2007. The R book. John Wiley and Sons Ltd, London, UK.

Dickson, A. G. 1990. Thermodynamics of the dissociation of boric acid in synthetic seawater from 273.15 to 298.15 K. Deep-Sea Res. **37**: 755–766. doi:10.1016/0198-0149(90)90004-F

Dickson, A. G., C. L. Sabine, A. G. Dickson, C. L. Sabine, and J. R. Christian. 2007. Guide to best practices for ocean CO_2 measurements, PICES special publication 3, IOCCP report No. 8.

Dickson, A. G. 2010. The carbon dioxide system in seawater: equilibrium chemistry and measurements. Guide to best practices for ocean acidification research and data reporting (Riebesell U, Fabry VJ, Hansson L, Gattuso JP, Eds.). 17–40.

Dove, S. G., D. I. Kine, O. Pantos, F. E. Angly, G. W. Tyson, and O. Hoegh-Guldberg. 2013. Future reef decalcification under business-as-usual CO_2 emission scenario. Proc. Natl. Acad. Sci. USA **110**: 15342–15347. doi:10.1073/pnas.1302701110

Ellison, S. L., M. Rosslein, and A. Williams. 2012. Quantifying uncertainty in analytical measurement. *In* Quantifying uncertainty in analytical measurement. Eurachem.

Fabry, J. F., B. A. Seibel, R. A. Feely, and J. C. Orr. 2008. Impacts of ocean acidification on marine fauna and ecosystem Processes. ICES J. Mar. Sci. **65**: 414–432. doi:10.1093/icesjms/fsn048

Fangue, N. A., M. J. O'Donnell, M. A. Sewell, P. G. Matson, A. C. MacPherson, and G. E. Hofmann. 2010. A laboratory-based, experimental system for the study of ocean acidification effects on marine invertebrate larvae. Limnol. Oceanogr. **8**: 441–452. doi:10.4319/lom.2010.8.441

Gattuso, J. P., and H. Lavigne. 2009. Technical note: Approaches and software tools to investigate the impact of ocean acidification. Biogeosciences **6**: 2121–2133. doi:10.5194/bg-6-2121-2009

Gattuso, J. P., I. E. Hendriks, and P. G. Brewer. 2014. Free-ocean CO_2 enrichment (FOCE) systems: Present status

and future developments. Biogeosciences **11**: 4057–4075. doi:10.5194/bg-11-4057-2014

Gibson, T. L., A. S. Abdul, and P. D. Chalmer. 1998. Enhancement of *in situ* bioremediation of BTEX-contaminated ground water by oxygen diffusion from silicone tubing. Ground Water Monit. Remediat. **18**: 93–104. doi:10.1111/j.1745-6592.1998.tb00606.x

Guadayol, O., N. J. Silbiger, M. J. Donahue, and F. I. M. Thomas. 2014. Patterns in temporal variability of temperature, oxygen and pH along an environmental gradient in a coral reef. PLoS One **9**: e85213. doi:10.1371/journal.pone.0085213

IPCC. 2014. Climate Change 2014: Synthesis Report. *In* Core Writing Team, R. K. Pachauri and L. A. Meyer [eds.], Contribution of working groups I, II and III to the fifth assessment report of the intergovernmental panel on climate change. IPCC, Geneva, Switzerland.

Jokiel, P. L. 2013. Coral reef calcification: Carbonate, bicarbonate and proton flux under conditions of increasing ocean acidification. Proc. R. Soc. B. **280**: 2013–0031.

Jokiel, P. L., K. D. Bahr, and K. U. S. Rodgers. 2014. Low-cost, high-flow mesocosm system for simulating ocean acidification with CO_2 gas. Limnol. Oceanogr.: Methods **12**: 313–322. doi:10.4319/lom.2014.12.313

Kayanne, H., and others. 2005. Seasonal and bleaching-induced changes in coral reef metabolism and CO_2 flux. Glob. Biogeochem. Cycles **19**. 1–11. doi:10.1029/2004GB002400

Khatiwala, S., and others. 2013. Global ocean storage of anthropogenic carbon. Biogeosciences **10**: 2169–2191. doi:10.5194/bg-10-2169-2013

Koch, M., G. Bowes, C. Ross, and X. H. Zhang. 2013. Climate change and ocean acidification effects on seagrasses and marine macroalgae. Glob. Change Biol. **19**: 103–132. doi:10.1111/j.1365-2486.2012.02791.x

Kroeker, K. J., R. L. Kordas, R. N. Crim, and G. G. Singh. 2010. Meta-analysis reveals negative yet variable effects of ocean acidification on marine organisms. Ecol. Lett. **13**: 1419–1434. doi:10.1111/j.1461-0248.2010.01518.x

Kroeker, K. J., and others. 2013. Impacts of ocean acidification on marine organisms: Quantifying sensitivities and interaction with warming. Glob. Change Biol. **19**: 1884–1896. doi:10.1111/gcb.12179

Leonardos, N. 2008. Physiological steady state of phytoplankton in the field? An example based on pigment profile of *Emiliania huxleyi* (Haptophyta) during a light shift. Limnol. Oceanogr. **53**: 306–311. doi:10.4319/lo.2008.53.1.0306

Leonardos, N., and R. J. Geider. 2005. Elevated atmospheric carbon dioxide increases organic carbon fixation by Emiliania huxleyi (Haptophyta), under nutrient-limited high-light conditions. J. Phycol. **41**: 1196–1203. doi:10.1111/j.1529-8817.2005.00152.x

Lueker, T. J., A. G. Dickson, and C. D. Keeling. 2000. Ocean pCO_2 calculated from dissolved inorganic carbon, alkalinity, and equations for K 1 and K 2: Validation based on laboratory measurements of CO 2 in gas and seawater at equilibrium. Mar. Chem. **70**: 105–119. doi:10.1016/S0304-4203(00)00022-0

Moya, A., and others. 2008. Calcification and associated physiological parameters during a stress event in the scleractinian coral Stylophora pistillata. Comp. Biochem. Physiol. **151**: 29–36. doi:10.1016/j.cbpa.2008.05.009

Pierrot, D. E. L., and D. W. R. Wallace. 2006. MS Excel Program Developed for CO2 System Calculations. ORNL/CDIAC-105a. Carbon Dioxide Information Analysis Center, Oak Ridge National Laboratory, U.S. Department of Energy, Oak Ridge, Tennessee, doi:10.3334/CDIAC/otg.CO2SYS_XLS_CDIAC105a.

R_Development_Core_Team. 2011. R: A language and environment for statistical computing. Available from http://www.R-project.org

Reynaud, S., N. Leclercq, S. Romaine-Lioud, C. Ferrier-Pagés, J. Jaubert, and J. P. Gattuso. 2003. Interacting effects of CO_2 partial pressure and temperature on photosynthesis and calcification in a scleractinian coral. Glob. Change Biol. **9**: 1660–1668. doi:10.1046/j.1365-2486.2003.00678.x

Richier, S., and others. 2014. Phytoplankton responses and associated carbon cycling during shipboard carbonate chemistry manipulation experiments conducted around Northwest European shelf seas. Biogeosciences **11**: 4733–4752. doi:10.5194/bg-11-4733-2014

Riebesell, U., V. J. Fabry, L. Hansson, J.-P. Gattuso [eds.]. 2010. Guide to best practices for ocean acidification research and data reporting. Publications Office of the European Union, 260 p.

Riebesell, U., and J. P. Gattuso. 2015. Lessons learned from ocean acidification research. Nat. Clim. Change **5**: 12–14. doi:10.1038/nclimate2456

Sciandra, A., and others. 2003. Response of coccolithophorid Emiliania huxleyi to elevated partial pressure of CO_2 under nitrogen limitation. Mar. Ecol. Prog. Ser. **261**: 111–123. doi:10.3354/meps261111

Smith, S., and D. Kinsey. 1978. Calcification and organic carbon metabolism as indicated by carbon dioxide. *In* D. Stoddart and R. Johannes [eds.], Coral reefs: Research methods. Monographs on oceanographic methodology. UNESCO.

Stewart, R. I., and others. 2013. Mesocosm experiments as a tool for ecological climate-change research. Adv. Ecol. Res. **48**: 71–181. doi:10.1016/B978-0-12-417199-2.00002-1

Suggett, D. J., and others. 2012. Sea anemones may thrive in a high CO_2 world. Glob. Change Biol. **18**: 3015–3025. doi:10.1111/j.1365-2486.2012.02767.x

Suggett, D. J., L. F. Dong, T. Lawson, E. Lawrenz, L. Torres, and D. J. Smith. 2013. Light availability determines susceptibility of reef building corals to ocean acidification. Coral Reefs **32**: 327–337. doi:10.1007/s00338-012-0996-7

Talmage, S. C., and C. J. Gobler. 2009. The effects of elevated carbon dioxide concentrations on the metamorphosis, size, and survival of larval hard clams (Mercenaria mercenaria), bay scallops (Argopecten irradians), and Eastern oysters (Crassostrea virginica). Limnol. Oceanogr. **54**: 2072–2080. doi:10.4319/lo.2009.54.6.2072

Tamburic, B., C. R. Evenhuis, D. J. Suggett, A. W. Larkum, J. A. Raven, and P. J. Ralph. 2015. Gas transfer controls carbon limitation during biomass production by marine microalgae. Chem. Sus. Chem. **8**: 2727–2736. doi: 10.1002/cssc.201500332

UNESCO. 1983. Algorithms for computation of fundamental properties of seawater. UNESCO Tech. Mar. Sci. **44**: 1–55.

Uppström, L. R. 1974. The boron/chlorinity ratio of deep-sea water from the Pacific Ocean. Deep Sea Res. **21**: 61–162.

Weiss, R. F., and B. A. Price. 1980. Nitrous oxide solubility in water and seawater. Mar. Chem. **8**: 347–359. doi:10.1016/0304-4203(80)90024-9

Weiss, R. F. 1974. Carbon dioxide in water and seawater: The solubility of a non-ideal gas. Mar. Chem. **2**: 203–215. doi:10.1016/0304-4203(74)90015-2

Yamamoto, S., H. Kayanne, M. Terai, A. Watanabe, K. Kato, A. Negishi, and K. Nozaki. 2012. Threshold of carbonate saturation state determined by CO_2 control experiment. Biogeosciences **9**: 1441–1450. doi:10.5194/bg-9-1441-2012

Zeebe, R. E., and D. Wolf-Gladrow. 2001. CO_2 in Seawater: Equilibrium, kinetics, isotopes. Elsevier.

Zuur, A. F., E. N. Leno, and C. S. Elphick. 2010. A protocol for data exploration to avoid common statistical problems. Methods Ecol. Evol. **1**: 3–14. doi:10.1111/j.2041-210X.2009.00001.x

Acknowledgments

We wish to thank Dr Phil Davey for help with the design and construction of the CO_2 probe and measurement system. Mr. Russell Smart is thanked for support in maintaining coral acclimation tanks and monitoring seawater chemistry. Prof Richard Geider is acknowledged for intellectual input. Funding for development of the MI-IRGA was provided to TL, DJSm and DJSu by the National Environmental Research Council UK (NERC grant NE/G020116/1), with additional support to DJSu from the ARC (Future Fellowship FT130100202) in preparation of the manuscript. The authors are grateful for continued support to work in the Cayman Islands from the Cayman Islands' Department of the Environment. Research conducted in the Cayman Islands was permitted by the Marine Conservation Board to EC. Finally, thank you to the three anonymous reviewers for their insightful comments that helped to improve upon an earlier version of the manuscript.

Conflict of Interest

None declared.

Submitted 02 June 2016
Revised 28 July 2016
Accepted 09 August 2016

Associate editor: Mike DeGrandpre